Journal of Integrative Agriculture 2026, 25(8): 3483–3494

Available online at ScienceDirect

Journal of Integrative Agriculture



RESEARCH ARTICLE

Asymbiotic biological nitrogen fixation makes a great contribution to nitrogen balance in unfertilized alpine grasslands across the Qinghai-Tibet Plateau

Ke Zhang[1], Feng Zhang[1], Yaoming Li[1#], Anna Du[1], Qingpu Wang[1], Zilong Liu[1], Fengcai He[1], Shengnan Wu[1], Shengmei Li[1], Chunhui Ma[1], Xianqi Zhou[1], Juejie Yang[1], Huaiying Yao[2], Richard D Bardgett[3], Shikui Dong[1#]

[1] *School of Grassland Science, Beijing Forestry University, Beijing 100083, China*
[2] *School of Environmental Ecology and Biological Engineering, Wuhan Institute of Technology, Wuhan 430205, China*
[3] *Department of Earth and Environmental Sciences, The University of Manchester, Manchester, M13 9PT, UK*

Highlights

- *Mesorhizobium* spp., known for their ability to fix nitrogen symbiotically, can also actively fix nitrogen in asymbiotic conditions.
- Asymbiotic nitrogen fixation results in ~0.50 Tg nitrogen input each year, which represents nearly 25% of the total nitrogen input in the Qinghai-Tibet Plateau grasslands.
- Soil properties, especially molybdenum concentration, are highlighted as the most significant factor affecting potential nitrogen fixation rates.

Abstract

Nitrogen limitation has been well documented in grasslands on the Qinghai-Tibet Plateau (QTP), significantly affecting predictions of plant growth and carbon sequestration potential under future climate change scenario. Beside atmospheric deposition, asymbiotic nitrogen fixation (ANF) may be crucial for nitrogen input in QTP grasslands, due to the lack of artificial fertilization and legume plants. However, little is known about the ANF's contribution to nitrogen input on the QTP. To fill this knowledge gap, we studied the composition, diversity and activity of ANF diazotrophs across the QTP grasslands by using multiple methods of transect sampling, ^{15}N-labeling and DNA stable isotope probing (SIP), amplicon sequencing, Random Forest algorithm modelling and digital mapping. We found that *Skermanella* and *Mesorhizobium* were the most abundant diazotrophic genera. Soil pH and total phosphorus concentration were the dominant driving factors for their composition and diversity. DNA stable isotope probing with $^{15}N_2$ revealed that *Mesorhizobium* were the most active nitrogen-fixing microorganisms. The potential N-fixation rates of these diazotrophs ranged from 0 to 18.1 kg N ha^{-1} yr^{-1}, resulting in an estimated annual input of approximately 0.50 Tg N across the entire QTP's alpine grasslands (i.e., ~25% of annual nitrogen input). The most important factor affecting the ANF rate was soil micronutrient molybdenum, a cofactor in the nitrogen-fixing nitrogenase, accounting for 24.64% of the variance. These findings suggested that ANF diazotrophs play important roles in maintaining nitrogen balance in the QTP grasslands and expand our understanding of *Mesorhizobium*'s ecological roles beyond traditional symbiotic interactions.

Keywords: alpine grasslands, asymbiotic nitrogen fixation, diazotrophs, DNA stable isotope probing, nitrogen input

1. Introduction

Increased plant growth and productivity of the alpine grassland on the Qinghai-Tibet Plateau (QTP), the largest alpine biome and alpine ecosystem in the world, has been observed since the 1980s, with predictions of further increases due to the region's warming and wetting climate

Received 22 May 2025; Received in revised form 23 July 2025; Accepted 26 August 2025; Available online 26 September 2025
Ke Zhang, Mobile: +86-19800322120, E-mail: zkcoral@bjfu.edu.cn; #Correspondence Yaoming Li, Mobile: +86-13401064151, E-mail: yaomingli@bjfu.edu.cn; Shikui Dong, Mobile: +86-13811445835, E-mail: dongshikui@bjfu.edu.cn

© 2026 CAAS. Publishing services by Elsevier B.V. on behalf of KeAi Communications Co. Ltd. This is an open access article under the CC BY-NC-ND license (http://creativecommons.org/licenses/by-nc-nd/4.0/). Peer review under responsibility of Editorial Board of *Journal of Integrative Agriculture*.
doi: 10.1016/j.jia.2025.09.031

(Chen *et al.* 2022). A crucial aspect of these projections is the availability of nitrogen, a key nutrient that supports plant growth (Davies-Barnard and Friedlingstein 2020). Nitrogen limitation on alpine vegetation growth has been robustly documented through analysis of soil and plant $\delta^{15}N$ along a ~3,000 km transect across the QTP during the 2000s and 2010s (Kou *et al.* 2020). Historically, anthropogenic nitrogen inputs to this region are negligible (Wang *et al.* 2017) and the atmospheric deposition rate was estimated at ~1.29 Tg N yr^{-1}. However, nitrogen losses were estimated at 1.10 Tg N yr^{-1}, largely due to NH_3 and NO_x emissions, erosion, and livestock grazing (Wang *et al.* 2023; Xiao *et al.* 2025), which nearly offset the nitrogen inputs through atmospheric deposition. Nitrogen-limited ecosystems have higher exogenous nitrogen demands (Aber *et al.* 1998; Zheng *et al.* 2020). Thus, biological nitrogen fixation (BNF) might play an important role in nitrogen inputs in the QTP's alpine grasslands. BNF occurs *via* two primary pathways: asymbiotic and symbiotic nitrogen fixation. Asymbiotic nitrogen fixation (ANF) has been found to contribute a greater proportion of nitrogen inputs than symbiotic pathway in many biomes (Reed *et al.* 2011), particularly those lacking large numbers of symbiotic nitrogen fixing plants. The biomass of legumes constitutes only 2.4–3.4% of alpine grasslands plants on the QTP (Jin *et al.* 2013). Correspondingly, the estimated symbiotic nitrogen fixation by these legume plants is ~0.23 Tg N yr^{-1} (Zong *et al.* 2020). Thus, ANF may be the key pathway of nitrogen inputs in the alpine grasslands of the QTP. However, the specific contribution of ANF, and the identity and activity of the microbial agents responsible, remain largely uncharacterized.

ANF is carried out by diverse diazotrophs (Pepe-Ranney *et al.* 2016), with fixation rates ranging from 0.1 to 21 kg N ha^{-1} yr^{-1} in temperate grasslands (Reed *et al.* 2011). The abundance, diversity and activity of diazotrophs vary significantly even within the same ecosystem, influenced by a range of environmental factors and non-linear response patterns (Tu *et al.* 2016; Wang *et al.* 2017). Various factors, including climate (Kou *et al.* 2019), topography (Petersen *et al.* 2012), soil physiochemical properties (Liang *et al.* 2010; Che *et al.* 2018; Kou *et al.* 2019), especially soil phosphorus and molybdenum (Jean *et al.* 2013), influence the spatial patterns of diazotroph activity and composition. The limitation of ANF by phosphorus is well-documented, especially in tropical ecosystems (Jean *et al.* 2013) when its concentration is less than 0.3 g kg^{-1} (Wurzburger *et al.* 2012). Average soil phosphorus content in the QTP's grasslands is ~0.4 g kg^{-1} (Wurzburger *et al.* 2012; Tan *et al.* 2021), indicating phosphorus might not be the primary limiting factor in constraining ANF here. Molybdenum is a key component of the most common nitrogenase enzyme and empirical evidence confirms Molybdenum limitation significantly constrains ANF in nutrient-poor tropical forest soils (Barron *et al.* 2009). Notably, QTP's grasslands exhibit substantially lower molybdenum compared to typical Chinese soil profiles (Zhang *et al.* 2010). This pronounced deficiency indicates molybdenum likely serves as a key regulator of ANF dynamics across the QTP.

Characterization of N-fixation organisms is a crucial step towards understanding how ANF can help balance the nitrogen cycling of the alpine grasslands to cope with future climate change. To understand the contribution of ANF to nitrogen cycling and its associated microbial agents on the QTP, we sampled soils over two ~2,000 km transects across the QTP's grasslands and analyzed the structure and activity of diazotrophs with a ^{15}N-labeling approach. Specifically, we aimed to address the following research questions: 1) What are the soil ANF microorganisms and how are their composition and diversity distributed geographically across the QTP? 2) What is the potential ANF rate in the QTP's alpine grasslands, which environmental factors primarily influence it, and which microbial species are responsible for nitrogen fixation? 3) How much nitrogen is potentially input annually by ANF microorganisms in the QTP's alpine grasslands and to what extent they contribute to N balance?

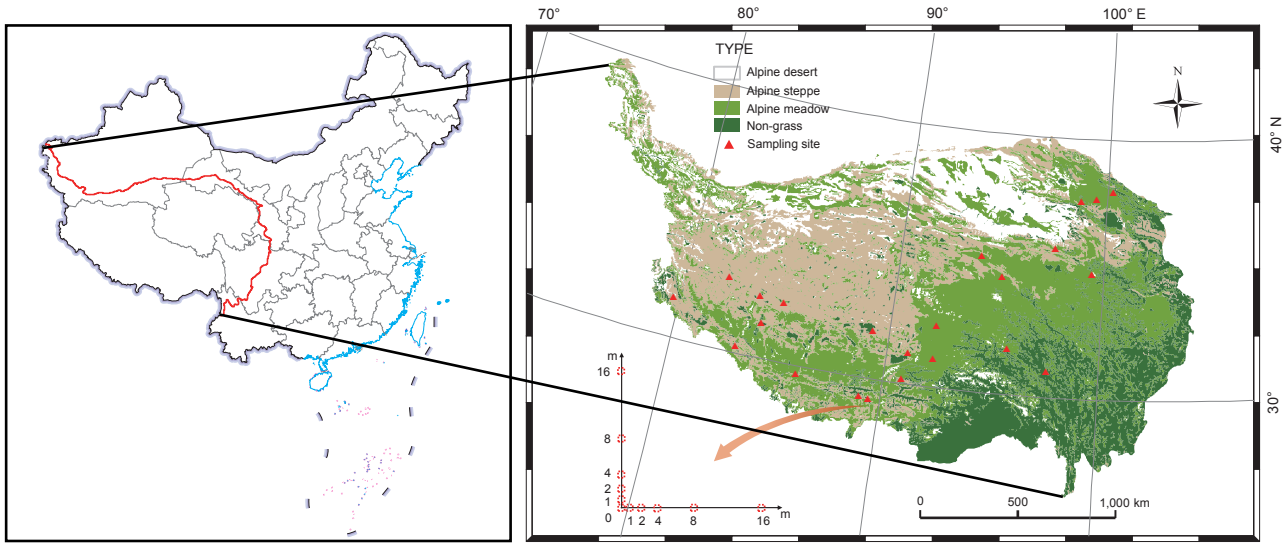
2. Materials and methods

2.1. Study sites and soil sampling

Study sites covered the whole QTP, where the alpine grasslands (mainly alpine meadow and alpine steppe) cover ~62% of the total region. We conducted soil sampling along transverse and longitudinal transects across the QTP. Soil samples were collected from 23 grasslands with 12 alpine meadow sites and 11 alpine steppe sites on the QTP in August 2021 and 2022 (Fig. 1; Appendix A). The sampling sites were randomly selected with 40–240 km intervals over the QTP. At each site, 11 surface soil samples (0–10 cm) were collected with a 7 cm diameter auger using nested sampling design, totaling 253 samples. Then, soils were sieved to ≤2 mm at field moisture and divided into three subsamples (60 g each). One subsample was stored at air temperature during transport and then air-dried for the determination of soil physicochemical properties; the other two subsamples were kept at 4°C during transportation and stored at −80°C and 4°C in the laboratory for DNA extraction and N fixation rate measurement, respectively. The coordinates and elevation of each sampling site were recorded using GPS. The normalized difference vegetation index (NDVI), mean annual temperature (MAT), mean annual precipitation (MAP) and evapotranspiration (2010–2019) were obtained from Resource and Environment Science and Data Center (https://www.resdc.cn). Atmosphere inorganic nitrogen deposition was obtained from National Ecosystem China Science Data (http://www.nesdc.org.cn/). The dataset of net primary productivity (NPP) was accessed from the National Earth System Science Data Center, National Science & Technology Infrastructure of China (http://www.geodata.cn).

2.2. Soil physicochemical determination

Soil organic carbon (SOC) was determined by a total organic carbon analyzer (TOC-L CPN, Kyoto, Japan) using the high-temperature combustion method. Air-dried soil samples were pretreated with hydrochloric acid to remove inorganic carbon before direct combustion. Dissolved organic carbon (DOC) was extracted with 0.5 mol L^{-1} K_2SO_4 at a soil-to-water ratio of 1:4 (w/v). The filtrate was acidified and purged, then analyzed in non-purgeable organic carbon mode of the TOC-L



审图号 : GS 京 (2026) 0965 号

Fig. 1 The distribution of the sampling sites and method of sampling. The arrow points to the quadrat layout for each sampling site. The spacing between the squares represents the actual quadrat distance.

analyzer. Total nitrogen (TN) concentration was measured using an element analyzer (EA 3000, Langenselbold, Germany). The concentrations of ammonia nitrogen (NH_4^+-N) and nitrate nitrogen (NO_3^--N) were determined using 1 mol L^{-1} $CaCl_2$ extracts by a flow injection autoanalyzer (AACE, Berlin, Germany). Total phosphorus (TP), total potassium (TK), iron, molybdenum and vanadium were determined using an inductively coupled plasma optical emission spectrometer (ICP-OES, iCCP 6300, Waltham, USA) after acid digestion (e.g., HNO_3-HCl mixture) of solid samples, with matrix-matched calibration standards to minimize interference. Soil moisture was measured using the wet soil and dry soil weights. Soil pH and electrical conductivity were determined in a 1:5 (w/v) soil-water suspension with a pH meter and conductometer, respectively.

2.3. Soil DNA extraction and sequencing

Soil DNA was extracted from 0.5 g soil using a PowerSoil^R Pro Kit (QIAGEN GmbH, Hilden, Germany) following the manufacturer's instructions. After being quality-checked by agarose gel electrophoresis, soil DNA samples were sent to Magigene Ltd. (Guangdong, China) for real-time PCR, library preparation, and amplicon sequencing on the Illumina HiSeq 2500 platform.

The copies of prokaryotic 16S rRNA and *nifH* gene were quantified using a LineGene9600 Quantitative PCR Detection System (Bioer Technology, Hangzhou, China). The quantification was conducted with universal primer sets for the 16S rRNA gene (515F: 5′-GTGCCAGCMGCCGCGGTAA-3′; 806R: 5′-GGACTACHV GGGTWTCTAAT-3′) (Zhou *et al.* 2016) and *nifH* (*nifH*-F: 5′-AAAGGYGGWATCGGYAARTCCACCAC-3′; *nifH*-R: 5′-TGSGCYTTGTCYTCRCGATBGGCAT-3′) (Morales *et al.* 2010), respectively. The PCR amplification was carried out using the BioRad S1000 PCR instrument (Bio-Rad Laboratory, CA, USA). Amplified PCR products for *nifH* gene were sequenced on the Illumina paired-end platform with the instrument of NovaSeq 6000 (Illumina, San Diego, CA, USA).

The *nifH* gene amplicons were analyzed according to Rädecker *et al.* (2022). Briefly, sequencing primers were removed using the cutadapt plugin available in Quantitative Insights into Microbial Ecology 2 (QIIME 2, version 2020.2) (Bolyen *et al.* 2019). Sequence quality control and representative sequences and feature amplicon sequence variants (ASVs) table construction were conducted using QIIME 2 with the DADA2 plugin. ASVs not annotated as the *nifH* gene and the ones assigned to *nifH* paralogs not involved in N fixation (clusters IV&V) were excluded. After sequence filtering, 55,570 ASVs (22,095,548 reads) retained from 134,748 ASVs (24,682,990 reads) were identified as correct *nifH* genes. Finally, the filtered representative sequences and feature ASV table were imported to QIIME 2 for follow-up analyses. The diversity of diazotrophs was calculated with the rarefied ASV table. The representative sequences were queried against the curated *nifH* gene database from the Zehr Lab (version June 2017) (Heller *et al.* 2014).

2.4. Potential nitrogen fixation activity measurement using ^{15}N-labeling approaches

Asymbiotic nitrogen fixation potential rates were calculated based on net changes in the concentration of ^{15}N in soil incubated with $^{15}N_2$ gas (Gupta *et al.* 2014). Soil samples (equivalent to 6 g dry soil weight per sample) were weighed into 25 mL glass vials and soil moisture was adjusted to 60% water-holding capacity. Subsamples were pre-incubated at 25°C for 24 h to ensure a fully active microbial community, and vials were sealed with a butyl rubber stopper. The headspace gas was replaced with gaseous mixture (98 atom% $^{15}N_2$:UHP-O_2:UHP-He=78:10:12, v/v, Isotope, Wuhan, China), with five repetitions per site. The control group was subjected to the same experimental procedure except that

$^{15}N_2$ was replaced by $^{14}N_2$. Sealed vials were incubated for seven days at 25°C in the dark. Gas samples were extracted by a Luer lock syringe and soils dried at 60°C for 48 h. Soil samples were ground using a stainless-steel Mixer Mill MM 400 grinder (Retsch GmbH, Haan, Germany) before ^{15}N analysis. The atom% ^{15}N of samples was analyzed using a MAT253 stable isotope mass spectrometer (Finnigan MAT, Bremen, Germany). The potential ANF rates were calculated using the following equation (Bei *et al.* 2013):

$$\text{Potential ANF rates}=\frac{\text{atom\%}^{15}N_{excess}\ \text{soil}\times\text{TN soil}}{\text{atom\%}^{15}N_{excess}\text{gas}\times t} \quad (1)$$

where atom% $^{15}N_{excess}$ soil represents atom percent excess of soil sample against an unenriched reference soil sample, TN soil represents total nitrogen concentration in the soil sample, atom% $^{15}N_{excess}$ gas represents atom percent excess in the vial atmosphere, and t is the incubation time (seven days in our case). Surface soil bulk density extracted at each grid cell was used to convert rates from dry-mass basis to area basis.

2.5. DNA stable isotope probing (SIP) fractionation and amplicon sequencing

Incubated soil DNA was extracted according to the method described above. Isopycnic density gradient centrifugation of the extracted DNA was carried out to isolate "heavy" ^{15}N-DNA and "light" ^{14}N-DNA in the SIP microcosms (Buckley *et al.* 2007). SIP fractionation was performed according to the protocols described by Neufeld *et al.* (2007) with minor modifications. CsCl density gradients were formed in 5.1 mL polyallomer centrifuge tubes (Hitachi, Tokyo, Japan) filled with gradient buffer (0.1 mol L^{-1} Tris-HCl, pH 8; 0.1 mol L^{-1} KCl; 1.0 mmol L^{-1} EDTA), which contained 6.0 μg DNA and 1.725 g mL^{-1} CsCl. Then the mixture was ultracentrifuged at 190,000×g for 48 h at 20°C in vacuum in a Vti65.2 vertical rotor (Beckman Coulter, CA, USA). After centrifugation, nuclease-free water was injected into the top of the tube using a syringe pump generating 16 equal fractions of 300 μL. The density of each fraction was determined using an AR200 refractometer (Reichert, NY, USA), and then converted to buoyant density. The DNA fraction was diluted in 30 mL nuclease-free water after PEG 6000 precipitation and 70% (v/v) ethanol purification. The number of *nifH* gene copies in each fraction was determined by qPCR used before. Quantitative analysis of *nifH* variation in fractions with different buoyancy density, according to the displacement of *nifH* in different buoyancy density gradient zones, the position and enrichment degree of ^{15}N-DNA was accurately determined, and compared with the ^{14}N-DNA control group. The isolated ^{15}N-DNA and native ^{14}N-DNA in the SIP microcosms were subjected to *nifH* gene amplicon sequencing using the same method as described above. All the raw sequences in this study have been submitted to NCBI's SRA database under the accession number PRJNA1155600.

2.6. Digital mapping

The selective model of RF was applied to a regional scale of the QTP. Processing raster data of selective environmental variables was programmed in R language with the use of the "raster" package. Function "projectRaster" was used to transform the coordinate system of raster data into a common geographic coordinate system, World Geodetic System 1984. Functions "resample" and "mask" were performed to uniformize resolution and range of raster data, respectively. The environmental variable values extracted at each grid cell were calculated by the final RF model to obtain the predicted ANF rates. The grid map of ANF rates on the QTP was displayed in ArcGIS 10.3 using the Krasovsky 1940 Albers projection, with 1 km spatial resolution.

2.7. Data analysis

Diversity analysis Data analysis was conducted using statistical platform R (version 4.3.1). We calculated bacterial α-diversity by using species richness and Shannon diversity, and β-diversity by computing the Bray-Curtis distance between samples and their respective group centroid. Non-metric multidimensional scaling (NMDS) analysis was used to visualize the sample relationships across different treatments in overall community composition, using the "metaMDS" function of the vegan package.

Factors affecting diazotrophic community A total of 18 plant and soil variables were assessed to evaluate possible linkages between bacteria and these variables. Before linear analysis, all variables were checked for normality and collinearity. Model selection and multi-model averaging were conducted with the package "MuMIn" (García-Palacios *et al.* 2018). To assess the relative importance of the observed variables as drivers of the potential ANF rates, we calculated the relative effect of the estimates for each of the factors compared with the effect of all parameter estimates in the model (function "rdacca.hp"). The optimal model was obtained based on the minimum value of akaike information criterion (AIC) (function "dredge"). In the final optimal model, eight variables were retained, including MAP, microbial composition, TP, TN, pH, NH_4^+-N, iron, and molybdenum. Prior to constructing a structural equation modeling (SEM), we performed multiple linear regression analysis on observed climate and soil variables to form composite variables to reduce the complexity of the SEM (Tian *et al.* 2021). SEM was performed using AMOSS 26.0 (IBM SPSS Statistics). The fit of the final model was indicated by a nonsignificant χ^2 test ($P \geq 0.05$), Other fitted statistics included the high normed fit index (NFI>0.90), goodness of fit index (GFI>0.90), low root mean square error of approximation (RMSEA<0.05), and low AIC value.

Modeling based on Random Forest (RF) algorithm RF is an ensemble learning method based on decision tree analysis and is a powerful algorithm to develop a predictive model (Breiman 2001). In this study, 12 relevant environmental variables (i.e., SOC, TN, TP, soil moisture, soil pH, NPP, evapotranspiration, MAP, MAT, NDVI, inorganic nitrogen deposition, and electrical conductivity) were taken as essential predictor variables including soil, climate, and vegetation to predict ANF rates on the QTP. The predictive model was built using package "randomForest" from R statistical software (Segovia *et al.* 2020). As a relatively simple process of parameter

optimization, the RF model optimizes only two parameters. The number of decision trees (n_{tree}) and the split size of the variable subset (m_{try}) are the hyperparameters of RF that were tuned to optimize the model. The "randomForest" function was used to build the model with the default parameters (n_{tree}=500, m_{try}=p/3, where p is the number of predictor variables) (Probst *et al.* 2019). The global minima of error with the change in the number of decision trees was taken as the optimal number of decision trees. Model performance was evaluated by root-mean squared error (RMSE), coefficient of determination (R^2) and mean absolute error (MAE). We indicated the contribution of the explanatory variables to the model by IncNodePurity. The larger they were, the more important the variables were for the RF model (Rehman *et al.* 2016). Variable reduction processes were implemented according to Tian *et al.* (2022) with minor modifications. First, IncNodePurity was used to rank the predictor variables. We then built the model sequentially, each time removing the least-significant variable from the previous model until there was only one variable left. Finally, we computed the cross-validation error at each step of removing based on five repeats of 5-fold cross validation.

RMSE was used to select the optimal model using the minimum value. When m_{try} was 2, the RMSE reached a minimum, where the values of R^2 and MAE were 0.72 and 1.95 (Appendix B-a). 500 decision trees were selected as the model parameter based on the correlation plot between the model error and n_{tree} (Appendix B-b). Considering computational efficiency, m_{try}=2 and n_{tree}=500 were chosen in the following study. Twelve variables were ranked based on the variable importance by increase in node purity (IncNodePurity) in RF (Appendix C-a). Model performance using the strategy of non-recursive elimination of variables showed that when the predictors were reduced to four, the model performed best with the lowest cross-validation error (Appendix B-c). A partial dependence plot was used to visualize the modeled correlation between ANF rates and the important variables (Appendix C-b). We found that potential ANF rates increased with increasing MAT and TN but decreased with increasing MAP and pH which was supported by multi-model averaging analyses and SEM. Therefore, MAT, MAP, TN and pH were selected based on the variable importance by IncNodePurity. Based on these four identified important predictors, a random forest regression model for potential ANF rates was structured: potential ANF rate ~MAT+MAP+TN+pH (n=109, R^2=0.73, RMSE=2.43, MAE=1.87). TN, pH and soil bulk density in dataset of digital soil mapping products for the QTP were downloaded from National Tibetan Plateau/Third Pole Environment Data Center (https://data.tpdc.ac.cn).

Modeling based on multiple regression Model selection analysis in the R package "glmulti" was used to identify the important predictors of the potential ANF rates (Zhang *et al.* 2022). The present study employed a model selection analysis based on maximum likelihood estimation, which involved fitting all possible models that comprised the potential predictors. The assessment of the significance of each predictor was carried out by calculating the sum of Akaike weights for all candidate models that contained that predictor. This value served as an indicator of the overall support for each predictor across all potential models. To distinguish between crucial and non-crucial predictors, a threshold of 0.8 was utilized. We used R package "lm" to structure a multiple regression model for ANF rates based on the identified important predictors.

The importance of potential predictors is based on the sum of the Akaike weights derived from model selection using corrected AIC. Model selection analyses identified that MAT, SOC, TN, and MAP were the predictors that exceeded the 0.8 sum-of-akaike-weights cutoff, which showed that the best model describing potential ANF rates included these four predictors as important predictors (Appendix D). Based on these four identified important predictors, a multiple regression model for asymbiotic nitrogen fixation rates of the topsoil on the QTP was structured: potential ANF rate ~MAT+SOC+TN+MAP (n=104, R^2=0.40, P<0.0001). The validation in RMSE from the final multiple linear regression model was 6.86, much greater than that of the random forest model.

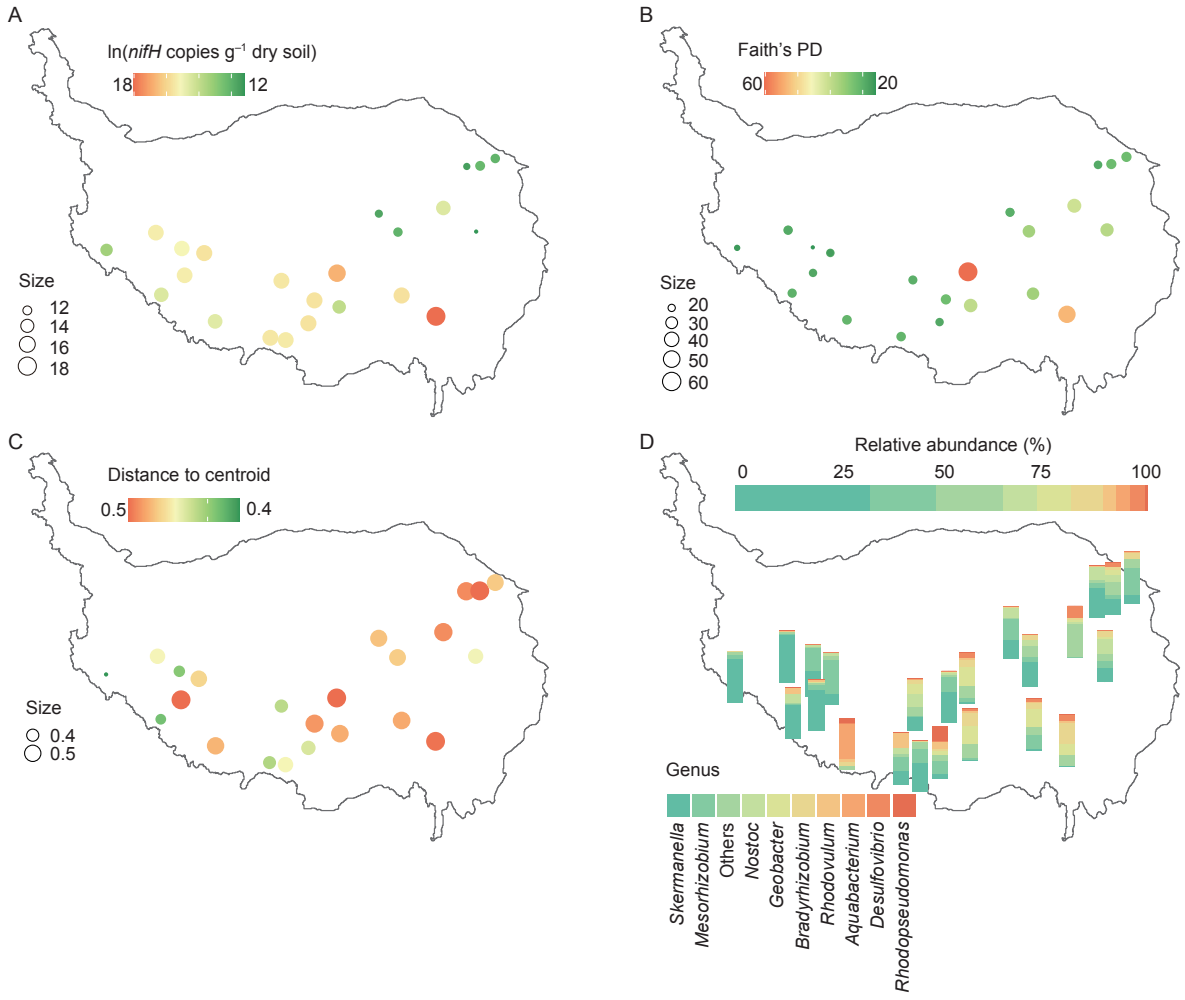
3. Results

3.1. Soil diazotrophs structure across the QTP's alpine grasslands

The soil properties were highly varied among the study sites (Appendix E-a). The soil diazotrophs in the QTP's grasslands were also highly numerous and diverse (Fig. 2; Appendices E-b and F). High variabilities of the *nifH* gene abundance values and their relative abundance to 16S rRNA gene with each group were detected, suggesting substantial spatial heterogeneity in *nifH* gene abundance (Fig. 2-A; Appendix F-a). From all the soil samples surveyed, a total of 78,055 unique sequences were obtained, which translated to 55,570 ASVs. Diazotrophic community showed higher alpha diversity (measured as species richness and Faith's phylogenetic diversity) in the southeast (Appendix F-b; Fig. 2-B) and higher beta diversity in the east (measured as distance to group centroid) (Fig. 2-C). In terms of community composition, soil diazotrophs were dominated by Alphaproteobacteria (59.81±27.17%, standard deviation, the same below) followed by Cyanobacteria and Deltaproteobacteria (Appendix F-c). *Skermanella* (33.24±27.96%), *Mesorhizobium* (17.72±18.66%), *Geobacter* (7.99±12.60%), *Nostoc* (8.63±9.86%) and *Bradyrhizobium* (6.99±9.69%) were the dominant genera of diazotrophs, and they accounted for more than 70% of the diazotrophic community members (Fig. 2-D). More than 90% of the *nifH* genes belonged to phylogenetic cluster I (Appendix F-d). Within cluster 1, cluster 1J was dominant in alpine grassland, followed by cluster 1K and 1B.

3.2. Nitrogen fixation rate and the corresponding active diazotrophs

Nitrogen fixation rate was converted into kg N ha^{-1} yr^{-1} based on half of the year's frost-free period and soil bulk density, representing an estimation of the annual potential contribution under favorable conditions. The average potential nitrogen



审图号：GS 京 (2026) 0965 号

Fig. 2 The geographical distribution patterns of abundance, composition and diversity of diazotrophs. A, copy numbers of the *nifH* gene. B, phylogenetic diversity (PD) of diazotrophic communities. C, beta diversity, measured as distance to group centroid of diazotrophic communities. D, composition of diazotrophic communities at genus level.

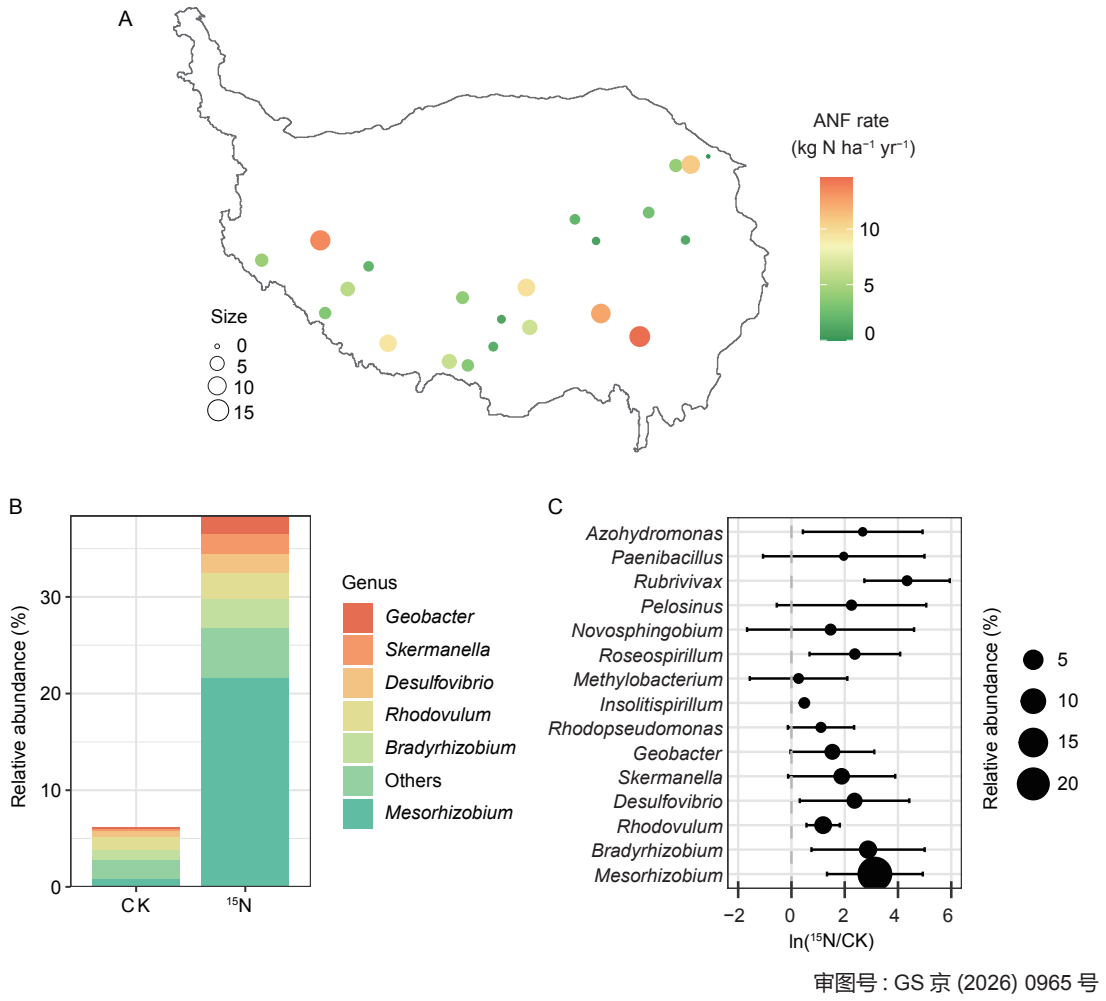
fixation rate was 5.42±4.53 kg N ha^{-1} yr^{-1}, with the highest rate in S18 (14.65±3.55 kg N ha^{-1} yr^{-1}) and the lowest rate in S23 (0 kg N ha^{-1} yr^{-1}) (Fig. 3-A; Appendix G-a). Most of the sampling sites had potential ANF rates below 10 kg N ha^{-1} yr^{-1}, except for sites S18, S2 (13.55±2.00 kg N ha^{-1} yr^{-1}), S17 (12.47±1.90 kg N ha^{-1} yr^{-1}), S22 (10.87±0.91 kg N ha^{-1} yr^{-1}).

Active diazotrophic species that incorporated ^{15}N into their DNA were detected by a differential change in their abundance within heavy gradient fractions of $^{15}N_2$-labeled samples relative to corresponding controls. Visible shift in DNA distribution along the buoyant density was detected (Appendix H), suggesting that the ^{15}N was assimilated by diazotrophs. A total of 265 ASVs were enriched in heavy fractions in $^{15}N_2$-labeled samples relative to corresponding controls and these ASVs were further identified as active diazotrophs (Appendix G-b). These active diazotrophs mostly belonged to *Mesorhizobium* (21.67±2.73%), *Bradyrhizobium* (3.04±0.32%), and *Rhodovulum* (2.76±0.41%) in $^{15}N_2$-labeled samples (Fig. 3-B and C; Appendix I).

3.3. Factors affecting diazotrophic community diversity and activity

More than 50% of the variation in diazotrophic community abundance, diversity and composition were explained by climate and soil properties. The abundance of the *nifH* gene showed a negative correlation with the soil iron concentration and plant net primary productivity and a positive correlation with MAT (Fig. 4-A). Diazotrophic species richness and Faith's phylogenetic diversity were negatively correlated with the concentrations of iron, DOC, and MAT and positively correlated with the concentration of TP, soil moisture, molybdenum, and MAP (Fig. 4-A). Soil pH was the key factor in impacting diazotrophic community composition (Fig. 4-A).

Soil molybdenum concentration was most important in controlling potential nitrogen fixation activity. As revealed by the multi-model averaging analyses, the model that included all abiotic and biotic predictors explained up to 63% (adjusted R^2) of the total variation observed in potential nitrogen fixation rates (Fig. 4-B). Climate factors (MAP), diazotrophic community composition and soil properties were responsible for 3.08,



审图号：GS 京 (2026) 0965 号

Fig. 3 Nitrogen fixation rate and the corresponding active diazotrophs. A, asymbiotic nitrogen fixation (ANF) rate. B, active diazotroph relative abundance. C, diazotrophic corresponding ln-fold changes for ^{15}N labeled versus control (^{14}N labeled) in heavy fractions.

14.60 and 45.33% of the explained variance, respectively. Soil properties (i.e., molybdenum, pH, TN, and TP) accounted for the highest percentage of explained variance, where molybdenum concentration, the most important one, explained 24.64% of the variation (Fig. 4-B).

The SEM showed direct and indirect contributions of each potential influential factor, including climate and soil properties, diazotrophic community diversity, composition and NPP to the potential N fixation rates, which explained 59% of the total variations (Fig. 4-C). The SEM further showed that soil properties were the dominant drivers of the potential nitrogen fixation rates, especially molybdenum concentration. Climate factors were also important drivers, not only because of their direct effects on nitrogen fixation rates but also *via* their indirect effects through NPP and soil properties (Fig. 4-C and D). Taken together, these two analyses jointly demonstrated that soil properties, especially molybdenum, played an important role in determining the potential nitrogen fixation rate in the alpine grassland of QTP.

3.4. Spatial patterns of potential nitrogen fixation rate and their contributions to nitrogen input on the QTP

Utilizing the selected optimal random forest model, potential nitrogen fixation rates in the topsoil of the QTP's grasslands were estimated and depicted on a map. The map revealed two key trends: firstly, potential nitrogen fixation rates were higher in the southeastern QTP and lower in the northwestern region (Fig. 5-A). Regionally, the average nitrogen fixation rate was estimated at 3.07 kg N ha^{-1} yr^{-1}. The minimum rate recorded was 1.62 kg N ha^{-1} yr^{-1} in the central QTP's alpine meadows, while the maximum rate was 12.98 kg N ha^{-1} yr^{-1} in the western QTP's alpine steppes (Fig. 5-A). Secondly, the distribution map indicated a patchy and interlaced pattern of nitrogen fixation across the alpine grasslands of the QTP. In the alpine meadows, potential rates varied from 1.62 to 12.98 kg N ha^{-1} yr^{-1}, averaging 2.97 kg N ha^{-1} yr^{-1} (Fig. 5-B). Meanwhile, in the alpine steppes, potential rates ranged from 1.65 to 12.98 kg N ha^{-1} yr^{-1}, with an average of 3.20 kg N ha^{-1} yr^{-1}, slightly exceeding that observed in the meadows (Fig. 5-C).

4. Discussion

4.1. Beyond symbiosis: rhizobium's key function in asymbiotic nitrogen fixation across the QTP

The natural eco-environments of alpine grasslands on the QTP harbor highly diverse and abundant diazotrophic

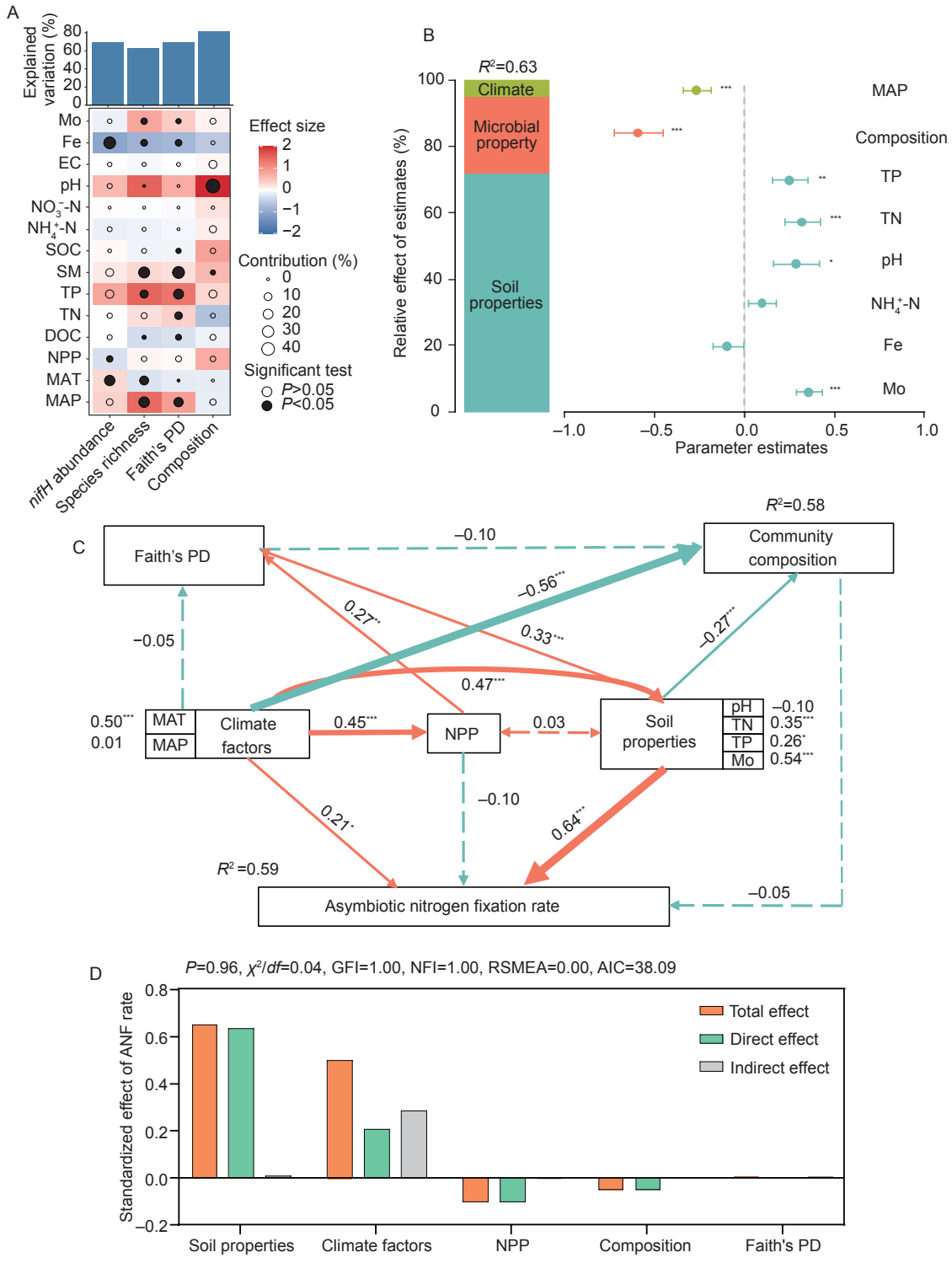
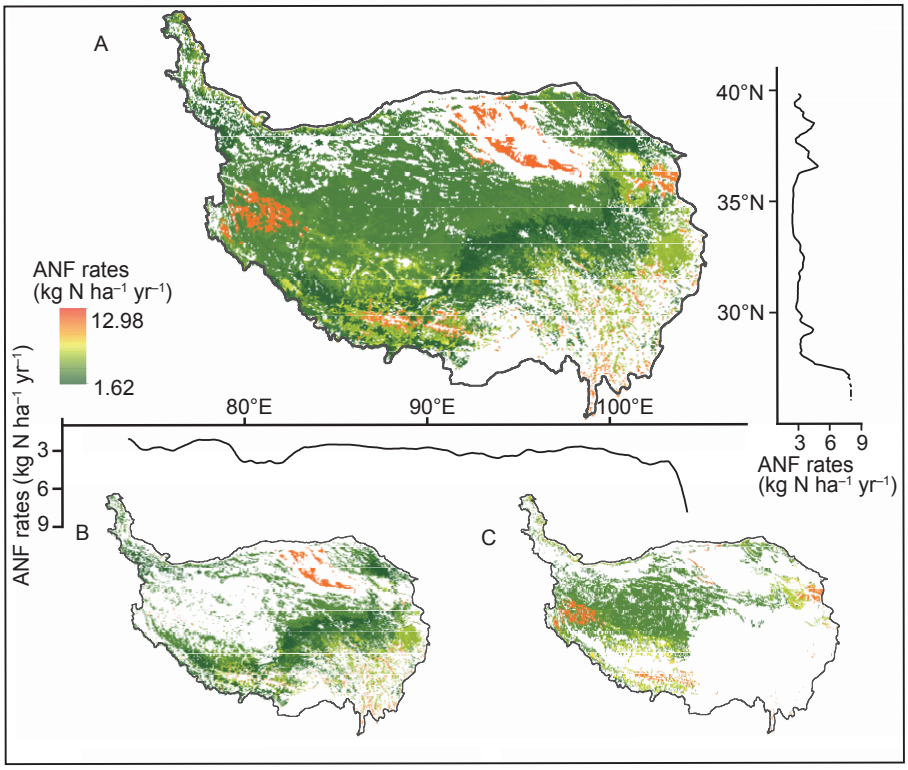


Fig. 4 Effects of climate and soil properties on diazotrophic communities. A, effect size of climate and soil properties on diazotrophic diversity, composition and the variations that can be explained by the climate and soil properties. The upper bar chart shows the overall explained variations by all the measured variables. The lower heatmap displays the relative influences of soil physicochemical properties and climate factors on the soil diazotrophs. B, relative effects of multiple predictors of potential asymbiotic nitrogen fixation (ANF) rates. It shows the relative importance of each predictor, expressed as the percentage of explained variance, as well as the average parameter estimates (standardized regression coefficients) of the model's predictors and their 95% confidence intervals. C, structural equation model showing the multivariate effects on potential ANF rates. Solid and dashed arrows represent significant and non-significant correlations, respectively, with red depicting positive correlations and blue negative correlations. The thickness of the arrow represents the strength of the correlations. The numbers adjacent to concrete predictors are standardized regression coefficients of the model's predictors. D, standardized effects of microbial community structure, soil properties, climate factors, and vegetation factor on asymbiotic nitrogen-fixation rates. Mo, molybdenum; Fe, iron; EC, electrical conductivity; SOC, soil organic carbon; SM, soil moisture; TP, total phosphorus; TN, total nitrogen; DOC, dissolved organic carbon; NPP, net primary productivity; MAT, mean annual temperature; MAP, mean annual precipitation; Faith's PD, Faith's phylogenetic diversity. *, $P<0.05$; **, $P<0.01$; ***, $P<0.001$.



审图号 : GS 京 (2026) 0965 号

Fig. 5 Spatial patterns of asymbiotic nitrogen-fixation rates on the Qinghai- Tibet Plateau with a resolution of 1 km. A, predicted spatial patterns of asymbiotic nitrogen-fixation rates in alpine grasslands. B, potential asymbiotic nitrogen-fixation rates in alpine meadows. C, potential asymbiotic nitrogen-fixation rates in alpine steppes. ANF, asymbiotic nitrogen fixation.

communities (Fig. 2; Appendix F). The abundance of diazotrophs in QTP's alpine grassland soils quantified with *nifH* gene was higher than the grasslands in New Zealand (Griffith *et al.* 2017) and Australia (Lindsay *et al.* 2010), but lower than Arctic tundra (Feng *et al.* 2019) and temperate meadows (Zhou *et al.* 2021). Alphaproteobacteria (60.63%) was the most abundant diazotroph in QTP alpine grassland soils, similar as agricultural grassland and forest soils (Pereira e Silva *et al.* 2013; Berthrong *et al.* 2014; Li *et al.* 2021). Their prevalence is likely due to Proteobacteria's adaptability to extreme environments (Liu *et al.* 2022). DNA-SIP with $^{15}N_2$ indicated that *Mesorhizobium*, *Bradyrhizobium*, and *Rhodovulum* were the most active genera in ANF. Generally, *Mesorhizobium* and *Bradyrhizobium* have been extensively characterized for their ability to fix nitrogen and enter the root hairs of legumes to form symbiotic nodules (Shamseldin *et al.* 2017). Our results indicated that their role in nitrogen fixation is far beyond traditional symbiotic relationships with legumes. The high ^{15}N-enrichment of these groups indicated that they were unlikely to absorb ^{15}N from other diazotrophs (cross-feeding). The fact that nitrogen fixation genes (*nif* and *fix*) are probably more ancient than nodulation genes (*nod* and *nol*) (Laranjo *et al.* 2014; Stüeken *et al.* 2015) may suggest that the nitrogen fixation ability of these genera is an ancient characteristic independent of nodulation. *Bradyrhizobium* is one of the most abundant species in soil and widely distributes in ecosystems lacking legumes (Uroz *et al.* 2010; Hartmann *et al.* 2012), indicating that symbiosis might not be its predominant lifestyle. Additionally, most of the detected diazotrophs was classified as Cluster I, predominantly composed of aerobic taxa. Other diazotrophs, such as *Skermanella*, *Geobacter* and *Desulfovibrio*, also showed a high ANF activity. The nitrogen fixation rate of these diazotrophs in QTP's grasslands was higher than tundra and boreal forest, but lower than temperate grasslands (Reed *et al.* 2011). Collectively, our results illustrated the geographical distribution pattern of the composition, diversity and function of the soil asymbiotic nitrogen-fixing microorganisms in the alpine grassland of the QTP. In addition, our findings highlighted the potential of asymbiotic *Mesorhizobium*, *Bradyrhizobium*, and *Rhodovulum* to contribute to ANF in the QTP's alpine grasslands.

4.2. Factors affecting diazotrophic community diversity and activity

Distinct diazotrophic community compositions and diversities in the grassland of the QTP were detected, due to the different environmental factors (Appendix E). Our study revealed that over 60% of variations in diazotrophic community diversity and composition were explained by climate and soil properties. Previous research has established that climate factors, particularly MAP, play considerable roles on diversity of diazotrophs across broad spatial scales (Che *et al.* 2018; Liu *et al.* 2024). And soil moisture is important in affecting diazotrophic community diversity. Moisture availability emerged as a critical driver, likely because diazotrophs prefer

anoxic microenvironments created by high moisture levels, which prevent inhibition of nitrogenase activity by oxygen (Smercina *et al.* 2019). Moreover, the concentration of phosphorus, which is crucial for the ATP-demanding process of nitrogen fixation (Raven 2012), was significantly positive correlated with diazotrophic diversity. Phosphorus-replete environments notably enhance the energy transduction efficiency of diazotrophs, permitting the persistence of more species. Surprisingly, despite the iron dependent nature of nitrogen fixation, the soil iron concentration was negatively correlated with diazotrophic abundance and diversity. This negative correlation might be due to the negative correlation between iron and molybdenum availability. Molybdenum was identified as critical factor in affecting diazotrophic community (Barron *et al.* 2009). The main inorganic form of molybdenum in oxic soils is molybdate (MoO_4^{2-}), which can interact with iron oxides to drastically reduce molybdenum bioavailability (Pasricha *et al.* 1997), especially under acidic conditions such as those found in alpine meadow (pH=6.3) here. Our results demonstrated significant pH-driven shifts in diazotrophic community diversity and composition in QTP's alpine meadow. These findings align with established literature documenting soil pH as a primary determinant of soil bacterial community (Lauber *et al.* 2009; Rousk *et al.* 2010; Fu *et al.* 2025). This pH-diversity relationship in diazotrophs may be interpreted in two ways. First, pH may directly regulate the community through differential population sensitivities. Second, pH often covaries with key factors like nutrients and vegetation. Therefore, the observed diversity pattern could also reflect the indirect and compounded effects of these co-varying environmental conditions, with pH acting as an integrated indicator.

Modeling approaches, including multi-model averaging and SEM, indicate that molybdenum significantly influences potential ANF rates, highlighting its importance in controlling potential ANF activity in alpine grassland ecosystems. This 24.64% independent explanatory power surpasses major climatic factors, reflecting molybdenum's unique biochemical function as the catalytic center of nitrogenase. This enzyme requires molybdenum within its iron-molybdenum cofactor to break inert N_2 bonds, a process demanding 16 ATP molecules per reaction (Durrant 2002). When molybdenum is scarce, diazotrophs cannot efficiently utilize energy for nitrogen fixation, forcing metabolic resources toward cellular maintenance instead. Alpine conditions intensify this constraint: persistent subzero temperatures slow microbial recycling of organic molybdenum pools; acidic condition reduces molybdenum bioavailability; and recurring freeze-thaw cycles physically trap molybdenum in soil aggregates. Our findings align with global evidence that molybdenum scarcity governs nitrogen fixation across ecosystems, from tropical forests to alpine grasslands (Barron *et al.* 2009; Reed *et al.* 2013). Future models must prioritize molybdenum bioavailability to accurately project nitrogen cycling under climate change.

4.3. New insights into nitrogen fixation fluxes in alpine grassland driven by machine learning

We employed multiple linear regression and random forest models to predict topsoil potential ANF rates across the Qinghai-Tibet Plateau. Cross-validation confirming the random forest's superior performance (higher R^2 and lower RMSE) (Appendix B), attributable to its ability to capture nonlinear interactions among predictors (e.g., MAP, TN, pH, and MAT; Appendix C-b). Critically, our modeling integrated direct ^{15}N labeling approach measurement, which is currently the most accurate method for measuring the potential nitrogen fixation rate. This method tracks actual N_2 molecule assimilation, avoiding systematic biases inherent in acetylene reduction assays that rely on arbitrary conversion factors. For validation, we compared our results with two typical data-based BNF estimates (Table 1). Cleveland *et al.* (1999) linked evapotranspiration with nonagricultural BNF, indicating a mean fixation rate of 3.25 kg N ha^{-1} yr^{-1} on QTP. Davies-Barnard and Friedlingstein (2020) provided a biome-upscaling approach that suggested a BNF rate of 4.60 kg N ha^{-1} yr^{-1}. However, these approaches may introduce global-scale biases due to single-factor dependencies and historical data scarcity. Integrating empirical ^{15}N data with this machine learning framework yielded an ANF estimate of 3.07 kg N ha^{-1} yr^{-1}.

The QTP comprises 1.35–1.75×10^6 km^2 of the alpine grasslands (Che *et al.* 2018; Chen W *et al.* 2022). Scaling our mean potential ANF rate (3.07 kg N ha^{-1} yr^{-1}) across this area gives an annual total of ~0.50 Tg N. Compared to atmospheric nitrogen deposition (~1.29 Tg N yr^{-1}) (Zhu *et al.* 2016), this represents a substantial input, equivalent to 39% of the atmospheric deposition and 25% of the total exogenous nitrogen inputs. Notwithstanding these advances, our study acknowledges the absence of controlled environmental gradient experiments to explicitly resolve factors interactions and to simulate the natural environment in the field. Future work should integrate such manipulative designs with process-based models. Such complementary approaches will refine predictions of nitrogen cycling under accelerating climate change. Our findings provide crucial insights into the diazotrophs responsible for BNF and the nitrogen input patterns in the alpine grasslands of the QTP, highlighting the potential for ANF to mitigating the pressure of enhanced nitrogen limitation due to increased vegetation biomass growth with a warming and wetting climate in the future.

Table 1 Comparison of biological nitrogen-fixation (BNF) rates between random forest method and previous methods on the Qinghai-Tibet Plateau (QTP)

Method	Scale	Mean BNF rate on QTP (kg N ha^{-1} yr^{-1})	Detail	Reference
Linear regression	Global	3.25	N fixation=0.234ET–0.172	Cleveland *et al.* (1999)
Upscaled biome	Global	4.60	IGBP land cover types	Davies-Barnard and Friedlingstein (2020)
Random forest	QTP	3.07		This study

5. Conclusion

This study quantified the ecological contribution of asymbiotic biological nitrogen fixation in alpine grasslands on the Qinghai-Tibet Plateau. It confirmed that genera such as Mesorhizobium can efficiently fix nitrogen under asymbiotic conditions. The total annual nitrogen fixation was approximately 0.50 Tg, accounting for 25% of the regional nitrogen input, making it the second largest nitrogen source after atmospheric deposition. The study also identified soil molybdenum concentration as the core limiting factor affecting nitrogen fixation rates, explaining nearly one quarter of the variation in nitrogen fixation. This research expands the understanding of the ecological functions of Mesorhizobium and provides key parameter support for simulating nitrogen cycling in alpine ecosystems and predicting vegetation productivity under future warming and wetting conditions.

Acknowledgements

This work was supported by the National Key Research and Development Program of China (2021YFE0112400 and 2023YFF1304303) and the National Natural Science Foundation of China (32361143870).

Declaration of competing interest

The authors declare that they have no conflict of interest.

Declaration of generative AI and AI-assisted technologies in the writing process

The authors declare that they did not use AI in the preparation and writing of this manuscript.

Appendices associated with this paper are available at https://doi.org/10.1016/j.jia.2025.09.031

References

Aber J, McDowell W, Nadelhoffer K, Magill A, Berntson G, Kamakea M, McNulty S, Currie W, Rustad L, Fernandez I. 1998. Nitrogen saturation in temperate forest ecosystems: Hypotheses revisited. *BioScience*, **48**, 921–934.

Barron A R, Wurzburger N, Bellenger J P, Wright S J, Kraepiel A M L, Hedin L O. 2009. Molybdenum limitation of asymbiotic nitrogen fixation in tropical forest soils. *Nature Geoscience*, **2**, 42–45.

Bei Q, Liu G, Tang H, Cadisch G, Rasche F, Xie Z. 2013. Heterotrophic and phototrophic $^{15}N_2$ fixation and distribution of fixed ^{15}N in a flooded rice-soil system. *Soil Biology and Biochemistry*, **59**, 25–31.

Berthrong S T, Yeager C M, Gallegos-Graves L, Steven B, Eichorst S A, Jackson R B, Kuske C R. 2014. Nitrogen fertilization has a stronger effect on soil nitrogen-fixing bacterial communities than elevated atmospheric CO_2. *Applied and Environmental Microbiology*, **80**, 3103–3112.

Bolyen E, Rideout J R, Dillon M R, Bokulich N A, Abnet C C, Al-Ghalith G A, Alexander H, Alm E J, Arumugam M, Asnicar F, Bai Y, Bisanz J E, Bittinger K, Brejnrod A, Brislawn C J, Brown C T, Callahan B J, Caraballo-Rodríguez A M, Chase J, Cope E K, *et al.* 2019. Reproducible, interactive, scalable and extensible microbiome data science using QIIME 2. *Nature Biotechnology*, **37**, 852–857.

Breiman L. 2001. Random forests. *Machine Learning*, **45**, 5–32.

Buckley D H, Huangyutitham V, Hsu S F, Nelson T A. 2007. Stable isotope probing with $^{15}N_2$ reveals rovel noncultivated diazotrophs in soil. *Applied and Environmental Microbiology*, **73**, 3196–3204.

Che R, Deng Y, Wang F, Wang W, Xu Z, Hao Y, Xue K, Zhang B, Tang L, Zhou H, Cui X. 2018. Autotrophic and symbiotic diazotrophs dominate nitrogen-fixing communities in Tibetan grassland soils. *Science of the Total Environment*, **639**, 997–1006.

Chen H, Ju P, Zhu Q, Xu X, Wu N, Gao Y, Feng X, Tian J, Niu S, Zhang Y, Peng C, Wang Y. 2022. Carbon and nitrogen cycling on the Qinghai-Tibetan Plateau. *Nature Reviews Earth & Environment*, **3**, 701–716.

Chen W, Wang J, Chen X, Meng Z, Xu R, Duoji D, Zhang J, He J, Wang Z, Chen J, Liu K, Hu T, Zhang Y. 2022. Soil microbial network complexity predicts ecosystem function along elevation gradients on the Tibetan Plateau. *Soil Biology and Biochemistry*, **172**, 108766.

Cleveland C C, Townsend A R, Schimel D S, Fisher H, Howarth R W, Hedin L O, Perakis S S, Latty E F, Von Fischer J C, Elseroad A, Wasson M F. 1999. Global patterns of terrestrial biological nitrogen (N_2) fixation in natural ecosystems. *Global Biogeochemical Cycles*, **13**, 623–645.

Davies-Barnard T, Friedlingstein P. 2020. The global distribution of biological nitrogen fixation in terrestrial natural ecosystems. *Global Biogeochemical Cycles*, **34**, e2019GB006387.

Durrant M C. 2002. An atomic-level mechanism for molybdenum nitrogenase. Part 1. Reduction of dinitrogen. *Biochemistry*, **41**, 13934–13945.

Feng J, Penton C R, He Z, Van Nostrand J D, Yuan M M, Wu L, Wang C, Qin Y, Shi Z J, Guo X, Schuur E A G, Luo Y, Bracho R, Konstantinidis K T, Cole J R, Tiedje J M, Yang Y, Zhou J. 2019. Long-term warming in alaska enlarges the diazotrophic community in deep soils. *mBio*, **10**, e02521.

Fu G, Zhang G, Zhou H. 2025. Effects of long-term experimental warming on phyllosphere epiphytic bacterial and fungal communities of four alpine plants. *Journal of Integrative Agriculture*, **24**, 799–814.

García-Palacios P, Gross N, Gaitán J, Maestre F T. 2018. Climate mediates the biodiversity-ecosystem stability relationship globally. *Proceedings of the National Academy of Sciences of the United States of America*, **115**, 8400–8405.

Griffith J C, Lee W G, Orlovich D A, Summerfield T C. 2017. Contrasting bacterial communities in two indigenous *Chionochloa* (Poaceae) grassland soils in New Zealand. *PLoS ONE*, **12**, e0179652.

Gupta V V S R, Kroker S J, Hicks M, Davoren C W, Descheemaeker K, Llewellyn R. 2014. Nitrogen cycling in summer active perennial grass systems in South Australia: Non-symbiotic nitrogen fixation. *Crop & Pasture Science*, **65**, 1044–1056.

Hartmann M, Howes C G, VanInsberghe D, Yu H, Bachar D, Christen R, Henrik Nilsson R, Hallam S J, Mohn W W. 2012. Erratum: Significant and persistent impact of timber harvesting on soil microbial communities in Northern coniferous forests. *ISME Journal*, **6**, 2320–2320.

Heller P, Tripp H J, Turk-Kubo K, Zehr J P. 2014. ARBitrator: A software pipeline for on-demand retrieval of auto-curated *nifH* sequences from GenBank. *Bioinformatics*, **30**, 2883–2890.

Jean M E, Phalyvong K, Forest-Drolet J, Bellenger J P. 2013. Molybdenum and phosphorus limitation of asymbiotic nitrogen fixation in forests of Eastern Canada: Influence of vegetative cover and seasonal variability. *Soil Biology and Biochemistry*, **67**, 140–146.

Jin D, Ma J, Ma W, Liang C, Shi Y, He J S. 2013. Legumes in Chinese natural grasslands: Species, biomass, and distribution. *Rangeland Ecology & Management*, **66**, 648–656.

Kou D, Yang G, Li F, Feng X, Zhang D, Mao C, Zhang Q, Peng Y, Ji C, Zhu Q, Fang Y, Liu X, Xu R, Li S, Deng J, Zheng X, Fang J, Yang Y. 2020. Progressive nitrogen limitation across the Tibetan alpine permafrost region. *Nature Communications*, **11**, 3331.

Kou Y, Li C, Li J, Tu B, Wang Y, Li X. 2019. Climate and soil parameters are more important than denitrifier abundances in controlling potential denitrification rates in Chinese grassland soils. *Science of the Total Environment*, **669**, 62–69.

Laranjo M, Alexandre A, Oliveira S. 2014. Legume growth-promoting rhizobia: An overview on the *Mesorhizobium* genus. *Microbiology Research*, **169**, 2–17.

Lauber C L, Hamady M, Knight R, Fierer N. 2009. Pyrosequencing-based assessment of soil pH as a predictor of soil bacterial community structure at the continental scale. *Applied and Environmental Microbiology*, **75**, 5111–5120.

Li W, Li F, Zeng H, Ma L, Qi L, Wang X, Wang W, Peng Z, Degen A A, Bai Y, Zhang T, Huang M, Han J, Shang Z. 2021. Diversity and variation of asymbiotic nitrogen-fixing microorganisms in alpine grasslands on the Tibetan Plateau. *Frontiers in Ecology and Evolution*, **9**, 702848.

Liang Y, Van Nostrand J D, Deng Y, He Z, Wu L, Zhang X, Li G, Zhou J. 2010. Functional gene diversity of soil microbial communities from five oil-contaminated fields in China. *ISME Journal*, **5**, 403–413.

Lindsay E A, Colloff M J, Gibb N L, Wakelin S A. 2010. The abundance of microbial functional genes in grassy woodlands is influenced more by soil nutrient enrichment than by recent weed invasion or livestock exclusion. *Applied and Environmental Microbiology*, **76**, 5547–5555.

Liu D, Song X, Hu J, Liu Y, Wang C, Henkin Z. 2024. Precipitation affects soil nitrogen fixation by regulating active diazotrophs and nitrate nitrogen in an alpine grassland of Qinghai-Tibetan Plateau. *Science of the Total Environment*, **919**, 170648.

Liu F, Wu H, Zhao Y, Li D, Yang J-L, Song X, Shi Z, Zhu A X, Zhang G L. 2022. Mapping high resolution national soil information grids of China. *Science Bulletin*, **67**, 328–340.

Morales S E, Cosart T, Holben W E. 2010. Bacterial gene abundances as indicators of greenhouse gas emission in soils. *ISME Journal*, **4**, 799–808.

Neufeld J D, Vohra J, Dumont M G, Lueders T, Manefield M, Friedrich M W, Murrell J C. 2007. DNA stable-isotope probing. *Nature Protocols*, **2**, 860–866.

Pasricha N S, Nayyar V K, Singh R P. 1997. *Molybdenum in Agriculture*. Cambridge University Press, Ottawa. pp. 245–270.

Pepe-Ranney C, Koechli C, Potrafka R, Andam C, Eggleston E, Garcia-Pichel F, Buckley D H. 2016. Non-cyanobacterial diazotrophs mediate dinitrogen fixation in biological soil crusts during early crust formation. *ISME Journal*, **10**, 287–298.

Pereira e Silva M C, Schloter-Hai B, Schloter M, van Elsas J D, Salles J F. 2013. Temporal dynamics of abundance and composition of nitrogen-fixing communities across agricultural soils. *PLoS ONE*, **8**, e74500.

Petersen D G, Blazewicz S J, Firestone M, Herman D J, Turetsky M, Waldrop M. 2012. Abundance of microbial genes associated with nitrogen cycling as indices of biogeochemical process rates across a vegetation gradient in Alaska. *Environmental Microbiology*, **14**, 993–1008.

Probst P, Wright M N, Boulesteix A L. 2019. Hyperparameters and tuning strategies for random forest. *Data Mining and Knowledge Discovery*, **9**, e1301.

Rädecker N, Pogoreutz C, Gegner H M, Cárdenas A, Perna G, Geißler L, Roth F, Bougoure J, Guagliardo P, Struck U, Wild C, Pernice M, Raina J-B, Meibom A, Voolstra C R. 2022. Heat stress reduces the contribution of diazotrophs to coral holobiont nitrogen cycling. *ISME Journal*, **16**, 1110–1118.

Raven J A. 2012. Protein turnover and plant RNA and phosphorus requirements in relation to nitrogen fixation. *Plant Science*, **188**, 25–35.

Reed S C, Cleveland C C, Townsend A R. 2011. Functional ecology of free-living nitrogen fixation: A contemporary perspective. *Annual Review of Ecology Evolution and Systematics*, **42**, 489–512.

Reed S C, Cleveland C C, Townsend A R. 2013. Relationships among phosphorus, molybdenum and free-living nitrogen fixation in tropical rain forests: Results from observational and experimental analyses. *Biogeochemistry*, **114**, 135–147.

Rehman A N, Kalyanaraman S, Ahmad T, Pervaiz F, Saif U, Subramanian L. 2016. Fine-grained dengue forecasting using telephone triage services. *Science Advances*, **2**, e1501215.

Rousk J, Bååth E, Brookes P C, Lauber C L, Lozupone C, Caporaso J G, Knight R, Fierer N. 2010. Soil bacterial and fungal communities across a pH gradient in an arable soil. *ISME Journal*, **4**, 1340–1351.

Segovia R A, Pennington R T, Baker T R, Coelho de Souza F, Neves D M, Davis C C, Armesto J J, Olivera-Filho A T, Dexter K G. 2020. Freezing and water availability structure the evolutionary diversity of trees across the Americas. *Science Advances*, **6**, eaaz5373.

Shamseldin A, Abdelkhalek A, Sadowsky M J. 2017. Recent changes to the classification of symbiotic, nitrogen-fixing, legume-associating bacteria: A review. *Symbiosis*, **71**, 91–109.

Smercina D N, Evans S E, Friesen M L, Tiemann L K. 2019. To fix or not To fix: Controls on free-living nitrogen fixation in the rhizosphere. *Applied and Environmental Microbiology*, **85**, e02546–18.

Stüeken E E, Buick R, Guy B M, Koehler M C. 2015. Isotopic evidence for biological nitrogen fixation by molybdenum-nitrogenase from 3.2 Gyr. *Nature*, **520**, 666–669.

Tan Q, Jia Y, Wang G. 2021. Decoupling of soil nitrogen and phosphorus dynamics along a temperature gradient on the Qinghai-Tibetan Plateau. *Geoderma*, **396**, 115084.

Tian P, Liu S, Zhao X, Sun Z, Yao X, Niu S, Crowther T W, Wang Q. 2021. Past climate conditions predict the influence of nitrogen enrichment on the temperature sensitivity of soil respiration. *Communications Earth & Environment*, **2**, 251.

Tian Z, Liu F, Liang Y, Zhu X. 2022. Mapping soil erodibility in southeast China at 250 m resolution: Using environmental variables and random forest regression with limited samples. *International Soil and Water Conservation Research*, **10**, 62–74.

Tu Q, Deng Y, Yan Q, Shen L, Lin L, He Z, Wu L, Van Nostrand J D, Buzzard V, Michaletz S T, Enquist B J, Weiser M D, Kaspari M, Waide R B, Brown J H, Zhou J. 2016. Biogeographic patterns of soil diazotrophic communities across six forests in the North America. *Molecular Ecology*, **25**, 2937–2948.

Uroz S, Buée M, Murat C, Frey-Klett P, Martin F. 2010. Pyrosequencing reveals a contrasted bacterial diversity between oak rhizosphere and surrounding soil. *Environmental Microbiology Reports*, **2**, 281–288.

Wang Y, Li C, Kou Y, Wang J, Tu B, Li H, Li X, Wang C, Yao M. 2017. Soil pH is a major driver of soil diazotrophic community assembly in Qinghai-Tibet alpine meadows. *Soil Biology and Biochemistry*, **115**, 547–555.

Wang Z H, Jiang Y, Zhang M H, Chu C J, Chen Y F, Fang S, Jin G, Jiang M, Lian J Y, Li Y, Liu Y, Ma K, Mi X, Qiao X, Wang X, Wang X, Xu H, Ye W, Zhu L, Zhu Y, *et al.* 2023. Diversity and biogeography of plant phyllosphere bacteria are governed by latitude-dependent mechanisms. *New Phytologist*, **240**, 1534–1547.

Wurzburger N, Bellenger J P, Kraepiel A M, Hedin L O. 2012. Molybdenum and phosphorus interact to constrain asymbiotic nitrogen fixation in tropical forests. *PLoS ONE*, **7**, e33710.

Xiao J, Dong S, Shen H, Zhang R, Shi H, He F, Li W, Li X, Li Y, Ding C. 2025. Short-term P addition may improve the stimulating effects of N deposition on N_2O emissions in alpine grasslands on the Qinghai-Tibet Plateau. *Journal of Integrative Agriculture*, **24**, 900–912.

Zhang B, Yang L, Wang W, Li Y, Li H. 2010. Quantification and comparison of soil elements in the Tibetan Plateau Kaschin-Beck disease area. *Biological Trace Element Research*, **138**, 69–78.

Zhang Y, Zhang F, Abalos D, Luo Y, Hui D, Hungate B A, García-Palacios P, Kuzyakov Y, Olesen J E, Jørgensen U, Chen J. 2022. Stimulation of ammonia oxidizer and denitrifier abundances by nitrogen loading: Poor predictability for increased soil N_2O emission. *Global Change Biology*, **28**, 2158–2168.

Zheng M, Chen H, Li D, Luo Y, Mo J. 2020. Substrate stoichiometry determines nitrogen fixation throughout succession in southern Chinese forests. *Ecology Letters*, **23**, 336–347.

Zhou J, Deng Y, Shen L, Wen C, Yan Q, Ning D, Qin Y, Xue K, Wu L, He Z, Voordeckers J W, Nostrand J D V, Buzzard V, Michaletz S T, Enquist B J, Weiser M D, Kaspari M, Waide R, Yang Y, Brown J H. 2016. Temperature mediates continental-scale diversity of microbes in forest soils. *Nature Communications*, **7**, 12083.

Zhou S, Xue K, Zhang B, Tang L, Pang Z, Wang F, Che R, Ran Q, Xia A, Wang K, Li L, Dong J, Du J, Hu R, Hao Y, Cui X, Wang Y. 2021. Spatial patterns of microbial nitrogen-cycling gene abundances along a precipitation gradient in various temperate grasslands at a regional scale. *Geoderma*, **404**, 115236.

Zhu J, Wang Q, He N, Smith M D, Elser J J, Du J, Yuan G, Yu G, Yu Q. 2016. Imbalanced atmospheric nitrogen and phosphorus depositions in China: Implications for nutrient limitation. *Journal of Geophysical Research* (Biogeosciences), **121**, 1605–1616.

Zong N, Song M, Zhao G, Shi P. 2020. Nitrogen economy of alpine plants on the north Tibetan Plateau: Nitrogen conservation by resorption rather than open sources through biological symbiotic fixation. *Ecology and Evolution*, **10**, 2051–2061.

Executive Editor-in-Chief Keke Yi
Managing Editor Lujuan Sun